ENHANCED FATIGUE CRACK DETECTION IN AGING AIRCRAFT USING CONTINUOUS ACOUSTIC EMISSION MONITORING

Stuart McBride, Yanhua Hong and Michael Pollard
Department of Physics
Royal Military College of Canada
Kingston, ON K7K 5L0

INTRODUCTION

During the past 20 years acoustic emission has been applied successfully to numerous materials degradation and failure problems. These applications are catalogued in Drouillard's bibliography of acoustic emission [1,2]. There have also been many disappointing results due to inadequate care and technique for discriminating between signals resulting from the materials degradation (or failure process of interest) and those resulting from environmental noise.

In the case of acoustic emission monitoring of airframes particular care has to be taken to discriminate between fatigue crack sources and noise. Routine measurements at randomly selected airframe locations show that the number of noise signals similar to crack advance signals during simulated flight test cyclic loading is typically in excess of 10^6 per hour of testing while the number of crack advance signals (if a crack is present) would be less than 1 per hour of testing. This is due to the presence of distributed noise sources throughout the structure which have signal features not unlike those of crack advance signals. I refer here to rubbing and fretting of bolted structural components, fasteners or crack faces. To solve this problem we have developed equipment which screens every detected signal by on-line windowing of a number of selectable signal parameters. The specific choice of on-line windowing parameters is made by the operator to take into account differences in acoustic behavior of the structure at different regions. Off-line windowing can also be applied on all recorded parameters after downloading the data to a portable computer directly or via modem to a computer in a remote location. Using this equipment and methodology crack face rubbing and crack advance signals can be discriminated from airframe noise provided the structure at the location of interest is acoustically calibrated and parametric windowing is then properly applied.

Acoustic emission can be used on-line as a continuous monitoring technique or alternatively as a periodic proof test. In either case the structure is required to be stressed to levels comparable to the highest in-service stress level. By this method it is possible to locate and identify sources such as fatigue cracks in a structure which is subject to complex loading during service. Indeed, acoustic emission can be used to determine the loading conditions and loading sequences under which fatigue crack growth takes place at each location in a large structure as well as providing a history of crack growth at each site during the monitoring period. In addition to providing such a diagnostic capability acoustic emission can detect fatigue cracks which cannot be detected readily and reliably by

Review of Progress in Quantitative Nondestructive Evaluation, Vol. 12
Edited by D.O. Thompson and D.E. Chimenti, Plenum Press, New York, 1993

conventional NDI due to the proximity of other interfaces. For example, the problem of detecting cracks in fastener holes can be solved using acoustic emission to monitor many fastener holes simultaneously without the removal of fasteners [3]. Reliable NDI confirmation of these defects requires the removal of fasteners. Indeed a major controversy in using acoustic emission in aircraft structures at this time is the inadequacy of current, practical NDI techniques to confirm the presence of fatigue cracks detected by acoustic emission. These inadequacies have been found for radiography, LPI, ultrasonics and eddy current as they are used in practise.

This work, which is part of a larger program to address the application of acoustic emission to the detection of cracks during flight [3,4,5,6,7], will describe the use of acoustic emission to detect fatigue cracks in a full-scale aircraft structure during ground durability and damage tolerance testing. Data is presented for about 3,000 equivalent flying hours of continuous monitoring and describes our progress during the past two years. Prior work in this project has been previously described by the authors [3]. Attention is focussed here on the relative effectiveness of periodic acoustic emission testing and continuous acoustic emission monitoring. Comparison of the acoustic emission results with those of conventional NDI are made.

EXPERIMENTAL

The Data Acquisition System

The 32 channel instrumentation system is based on the dual-channel acoustic emission system developed at the Royal Military College of Canada. This data acquisition system (commercially available from AEMS, Acoustic Emission Monitoring Services Inc., Gananoque, Ontario, Canada) was designed and constructed specifically for the recording and interpretation of acoustic emission data in the laboratory and during flight. The design is based on criteria derived from the RMC work of almost a decade in the area of acoustic emission monitoring during flight [3,4,5,6,7]. These studies established the importance of the difference in arrival time of an event at different locations, signal risetime, and the magnitude and variation of the applied stress at the time of occurrence of the event. All of these parameters are necessary to isolate crack-related events from other noise sources during dynamic loading of a large, dispersive structure and are recorded by the data acquisition system used here. To provide maximum flexibility, the data acquisition system is designed to use either an available 115/230 V, 47-440 Hz electrical supply or internal batteries.

The output of each of the piezoelectric sensor elements is amplified by a preamplifier with nominal gain of 40 dB. The resulting signal is buffered, logarithmically amplified and envelope followed. These operations are accomplished using signal conditioning modules custom-made for the purpose (Fig. 1a). The output of each envelope follower is separately fed into the digital data acquisition system where the times of pre-selected amplitude threshold crossings (6 dB apart) are recorded and the digitized peak amplitude detected by a sample and hold technique (Fig. 1b). The amplified load, strain gauge and accelerometer values are digitized by an A/D convertor, as required, and stored in memory.

All of the above data are compressed into an event record which includes the time of occurrence of the event at each sensor, the difference in arrival times at two sensors (Δt), event risetimes for 6 dB change in amplitude, event durations, event decay times and event peak amplitudes. The resulting data set is then extracted from the data acquisition system via an RS-232 interface, transferred by modem to the data analysis centre and stored on disk on an external computer. By using a data multiplexer, several 2-channel systems are operated in parallel to achieve multi-channel capability. Since each 2-channel system has a CPU there is no decrease in data acquisition rate as the number of channels is increased. Extensive screening of data, field analysis and interpretation can be carried out immediately on the remote host monitoring computer which is also used for remote control of all features of the multiplexed data acquisition systems. Final analysis and interpretation are accomplished using spreadsheet software. Table 1 lists the general specifications of the apparatus.

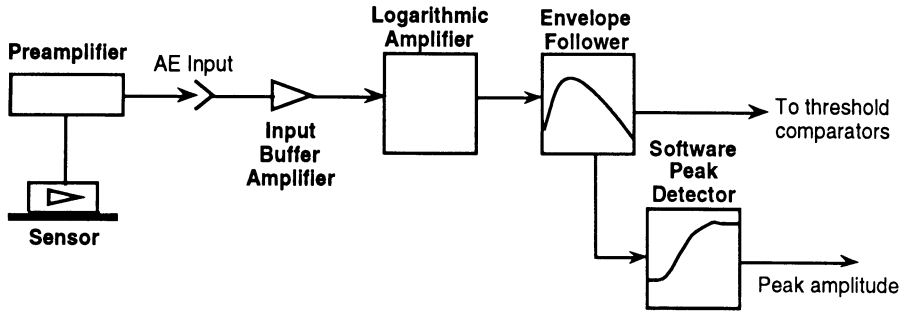

Fig. 1a. Schematic diagram of the AEMS acoustic emission signal conditioning.

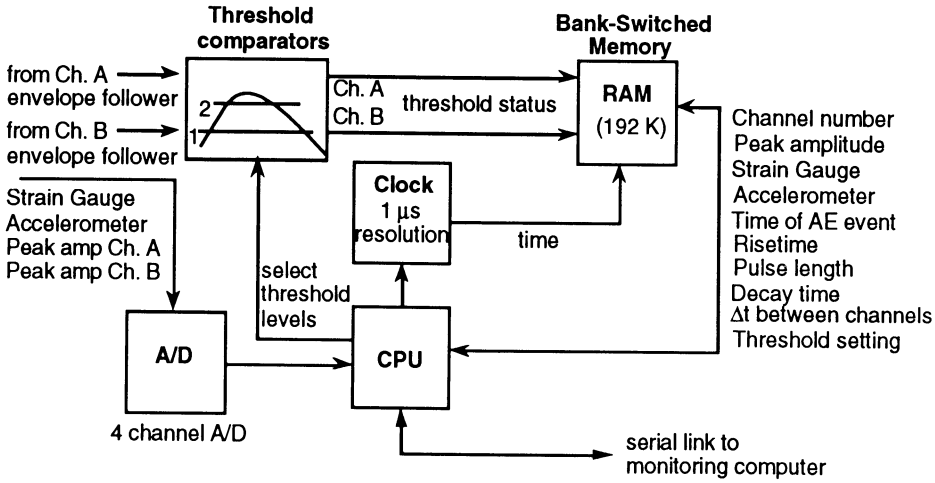

Fig. 1b. Schematic diagram of the AEMS acoustic emission data acquisition computer.

Monitored Regions

The regions monitored were selected by the fatigue test engineers and are located on the lower wing skin of a fighter aircraft. The particular areas of interest are the 15% spar regions between the indicated sensor locations and the 39% and 44% spar regions within the linear array of sensors as shown in Fig. 2. The precise location of each sensor is constrained by the presence of the pads which are used to transmit the simulated flight loads to the wing.

Table 1. General specifications for the AEMS digital data acquisition system for in-flight acoustic emission monitoring applications.

2 Channels AE	60 dB dynamic range
2 Analog Channels	10 V full-scale
Power Supply	115/230 V, 47-440 Hz or battery powered
Power Consumption	10 Watts maximum
Data Storage Capacity	192 or 384 Kbyte RAM with battery back-up
Dimensions	23 cm x 13.5 cm x 25 cm
Weight	2 kg
Mass Data Storage	External computer via RS-232 interface
Windowing on all recorded parameters	Available on-line and during post analysis

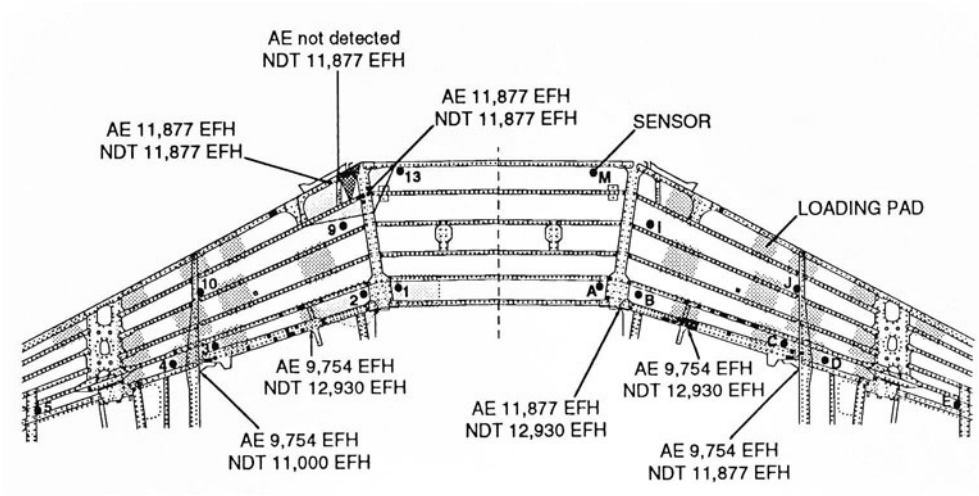

Fig. 2. Fatigue crack detection by continuous acoustic emission monitoring during 3,000 equivalent flying hours of full-scale testing. The numbers indicate the equivalent flying hours (EFH) at which acoustic emission detection or NDI confirmation took place. These defects occurred principally on the edge of the wing skin. Note that acoustic emission often detected the defect several thousands of equivalent flying hours before NDI confirmation was possible.

Wing Loading

Fatigue cycling loads were applied at various loading points to simulate the known flight load spectra measured on flying aircraft. The output of a strain gauge is recorded by the data acquisition system as the measure of the wing loading conditions at the time of occurrence of each acoustic emission signal. Table 2 lists the simulated flight load spectrum in terms of g and the normalized percent transverse strain relative to the value at 7g measured on the lower wing skin. The highest strain manoeuvres (6.5g and 7g) are of particular interest for the acoustic emission monitoring since they provide the highest loads, and hence, the most probable circumstances for crack advance acoustic emissions.

Acoustic Emission System Calibration

Pencil lead fracture was used to obtain the area calibration of the various acoustic emission parameters (Δt, pulse length, risetime, etc). It was found that, within the array, the difference in arrival time at neighbouring sensors is linear and results from an acoustic wave velocity of about 0.5 cm/μs. The measured risetime of the signals detected by the Dunegan Endevco D9202B sensors was less than 3μs and was essentially independent of source position between the sensors provided no abrupt changes in material thickness occurred. Such changes in the thickness usually involved additional fasteners to connect the wing skin to the substructure, and hence, introduced additional reflections.

Table 2. Number of occurrences of maximum g levels per thousand flying hours derived from measurements during typical flight conditions. Also shown is the % strain in the lower wing skin relative to the value at 7g.

g	Strain %	Loadings/10^3 Flying Hrs
4.5	64.3	1770
5.0	71.4	2828
5.5	78.6	1589
6.0	85.7	198
6.5	92.9	45
7.0	100.0	90

RESULTS AND DISCUSSION

Fig. 2 summarizes the defects detected in the lower wing skin of the full-scale test article by acoustic emission and confirmed by conventional NDI (eddy current and LPI). These defects are of two types:

(a) Fatigue cracks in fastener holes which were repaired at or before 9,754 equivalent flying hours of testing. Acoustic emission monitoring of these defects has been described and discussed previously [3].

(b) "New" defects detected during acoustic emission monitoring of a static load test at 9,754 equivalent flying hours prior to continuance of the ground durability and damage tolerance test or by continuous acoustic emission monitoring after the 9,754 equivalent flying hours major repair..

The "new" defects occurred principally at the wing skin edge aft of the 44% spar although one of the defects which was not detected by acoustic emission initiated at a fastener hole at the 15% spar. The 15% spar is that at the top edge of Fig. 2 while the 44% spar is that at the lower edge of Fig. 2. The reason why the 15% spar defect was not detected has been carefully analyzed. In order to detect this defect with the instrumentation in the configuration used, it would have to be sensed by sensor pairs 9/10 or 2/3. The sensitivity of sensor 10 for events originating at the undetected defect position was very low due to the wing skin geometry and substructure between the defect and sensor 10. This eliminated detection of that defect by the 9/10 sensor array. Further, during the monitoring period sensor 2 was acoustically bonded to the repair patch indicated in Fig. 2. This repair patch reduced the sensitivity of sensor 2 by about 20 dB thus preventing detection of the defect by array 2/3. Sensors 13 and M were thus added to improve detection in the critical 15% spar area by monitoring arrays 9/13 and I/M. No crack growth has been observed to date by these added arrays.

For each "new" defect the number of equivalent flying hours at which it was first detected by acoustic emission and confirmed by NDI respectively is given in Fig. 2. At the time of confirmation and repair the defects were of the order of 2 mm deep. A detailed assessment of each of the defects is being carried out using eddy current, ultrasonics, liquid penetrant inspection and sectioning of the material but was not available at the time of writing. Note that for a number of the defects acoustic emission detection preceded NDI detection by about 3000 equivalent flying hours which represents several years of normal operational use. In addition to the data presented here, other areas of the full-scale test article are also being monitored. These include the upper wing skin and vertical stabilizer skin. These data will be reported separately.

Fig. 3 shows the progress of the defect below sensor 3 in Fig. 2 during continuous acoustic emission monitoring. This defect which is located on the edge of the wing skin was first detected during a 7g static loading at 9,754 equivalent flying hours. NDI confirmation was not possible until 11,000 equivalent flying hours. Note however that the presence of the defect at 9,754 equivalent flying hours was established by examining acoustic emission signal features of less than ten maximum loading signals in two static test 7g loadings. Subsequent dynamic loading provided 124 7g loadings (Fig. 3). Fig. 4 shows a histogram of the number of crack advance signals per loading derived from the data of Fig. 3. It is seen that about 5 signals per loading is most probable although crack arrest could result in no detected crack advance during a particular 7g loading. The fracture face area of this defect was 20 mm^2 at the time of repair.

Fig. 5 shows the observed location of the defect using continuous monitoring and linear location. The velocity of sound in the wing skin in this vicinity is 0.5 cm/μs and the peak halfwidth is 16 μs resulting in a maximum zone location uncertainty of about ±2 cm. This location uncertainty is not unreasonable since the acoustic wavelength at 500 kHz is about 1 cm and the sensor diameters are each about 1.5 cm. It is clear from Fig. 5 that continuous monitoring during a large number of strain cycles provides a more accurate location than that which would be obtainable from a single test loading during a periodic

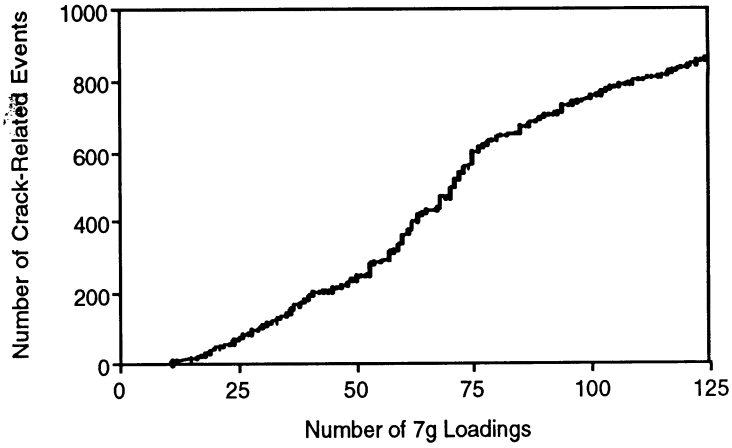

Fig. 3 Number of detected crack events as a function of the number of 7g loadings for the defect near sensor 3 (Fig. 2). Note the relatively large steps occurring between 7g loading number 50 and 7g loading number 75. This results from a particularly severe load spectrum in this range.

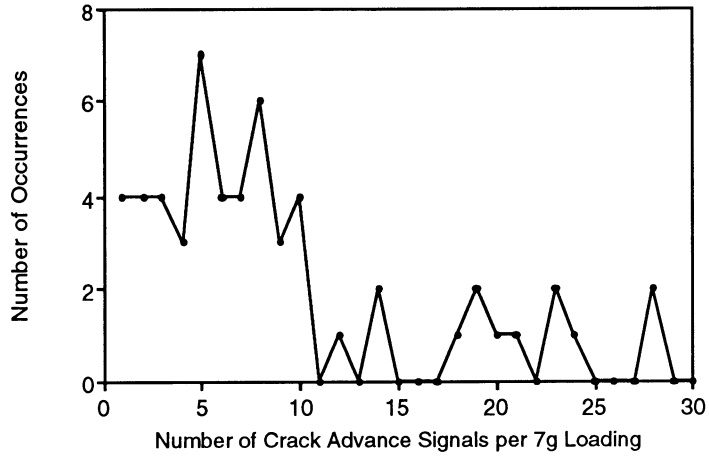

Fig. 4 Histogram for the number of crack advance events per 7g loading for the data of Fig. 3 (defect near sensor 3, Fig. 2). Note that the most probable number of events per 7g loading is about 5 although crack arrest can cause there to be 0 events in a given loading.

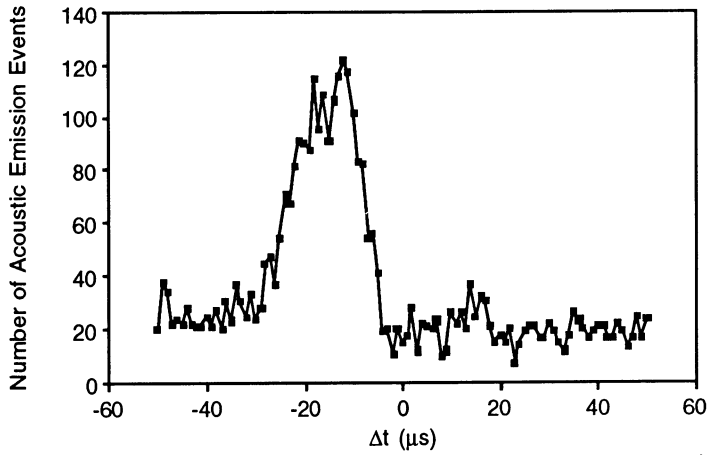

Fig. 5 Determination of crack site near sensor 3 (Fig. 2) by continuous acoustic emission monitoring. The measured acoustic velocity in the vicinity of this defect is 0.5 cm/μs and the halfwidth of the acoustic emission peak is 16 μs. Linear zone location of the source is to within ± 2 cm.

inspection. As shown in Fig. 3, if continuous acoustic emission monitoring is used the progressive growth of the fatigue crack can be plotted also as a function of the number of applied loading number. From this data it is clear that for 0<7g loading number <50 and for 75<7g loading number <125 the rate of crack advance is slower than for 50<7g loading number <75. This effect is real and results from the application of more frequent 7g loadings within the loading spectrum. This illustrates the efficacy of acoustic emission during programmable load cycling. Note also that the peak in Fig. 5 is readily distinguished from distributed structural noise resulting in the possible comparison of the crack advance signals with a laboratory database and the consequent reduction in ambiguity. This feature appears to result from the precise nature and location of the crack events compared to the more variable nature of the distributed structural rubbing sources.

CONCLUSIONS

Periodic testing involves analyzing the acoustic emission data from a test loading. It was found that the most probable number of crack advance events during a single loading is about five although temporary crack arrest may result in no crack advance data occurring during the test loading. Continuous monitoring on the other hand eliminates the possibility of an improper conclusion due to the effect of temporary crack arrest by increasing the number and frequency of "inspections" thereby increasing the number of crack advance events which are available for analysis. Detailed comparison of data with a laboratory database can then be used to confirm the type of source. In addition, continuous monitoring improves the location of crack advance sources and provides a better estimate of distributed structural noise.

ACKNOWLEDGEMENTS

The data acquisition and crack source location were carried out by AEMS Acoustic Emission Monitoring Services Inc., RR #2 Gananoque, Ontario, Canada, K7G 2V4 under contract to Supply and Services Canada. Supporting funds for the subsequent data analysis was provided to the Royal Military College of Canada by the Department of National Defence, Canada (ARP FUHDU and CRAD 144690RMC01). The ground durability and damage tolerance test and NDI measurements were conducted by Canadair, Montreal, under the supervision of Mr. G. Deziel, DAS Eng 6-3-4, National Defence Headquarters, Ottawa. The project was monitored by Major M. Brassard, DAS Eng 6-2, National Defence Headquarters, Ottawa, Ontario and Mr. W.R. Sturrock of the Materials Section, Defence Research Establishment - Pacific, Victoria, British Columbia .

REFERENCES

1. T. F. Drouillard, *Acoustic Emission, A Bibliography with Abstracts* (Plenum Data Company, New York, 1979).
2. T. F. Drouillard, *Bibliography Update* (J. Acoust. Emis., 1982-92).
3. S. L. McBride, M. R. Viner and M. D. Pollard, in Review of Progress in Quantitative NDE, Vol. 10B, edited by D. O. Thompson and D. E. Chimenti (Plenum Press, New York, 1991), p. 1913.
4. S. L. McBride and J. W. Maclachlan, J. Acoust. Emis. 1, p. 223 (1982).
5. S. L. McBride and J. W. Maclachlan, J. Acoust. Emis. 1, p. 229 (1982).
6. S. L. McBride and J. W. Maclachlan, J. Acoust. Emis. 3, p. 1 (1984).
7. S. L. McBride, M. D. Pollard, J. D. MacPhail, P. S. Bowman, and D. T. Peters, J. Acoust. Emis. 8, p. 4 (1989).